

Decoupling the Influence of Systemic Variables in the Peripheral and Cerebral Haemodynamics during ECMO Procedure by Means of Oblique and Orthogonal Subspace Projections*

A. Caicedo, Member, IEEE, I. Tachtsidis, M.D. Papademetriou, S. Van Huffel Fellow, IEEE

Abstract— Extra-Corporeal Membrane Oxygenation (ECMO) is a life support system for infants and children with cardio-respiratory failure. During ECMO it is possible to have unstable cerebral haemodynamics, due to strong oscillations in the systemic variables, among other factors, which may lead to brain damage in the patients. Therefore, monitoring the coupling between cerebral haemodynamics and systemic signals might alert us of possible imminent brain damage. In this study we explore the use of orthogonal and oblique subspace projections in the decoupling of these variables, by assessing the ratio between the projections of the haemodynamic variables, onto the subspace spanned by the systemic variables, and the original signals. The coupling of these two systems may differ as different protection mechanisms protect the peripheral system and the brain. Subspace projection was able to decompose the haemodynamic variables as a sum of components related to each systemic variable, separately. As expected, stronger coupling was found between the peripheral haemodynamic and the systemic variables.

I. INTRODUCTION

Extra-Corporeal Membrane Oxygenation (ECMO) procedure is a technique used to provide support for the heart and/or the lungs in patients with cardiac and/or respiratory failure. In veno-arterial (VA) ECMO patients are cannulated from

*This research was supported by: Research Council KUL: GOA MaNet, CoE EF/05/006 Optimization in Engineering (OPTEC), PFV/10/002 (OPTEC), IDO 08/013 Autism, several PhD/postdoc & fellow grants; Flemish Government:

FWO: PhD/postdoc grants, projects: FWO G.0302.07 (SVM), G.0341.07 (Data fusion), G.0427.10N (Integrated EEG-fMRI), G.0108.11 (Compressed Sensing) G.0869.12N (Tumor imaging) research communities (ICCoS, ANMMM); IWT: TBM070713-Accelero, TBM070706-IOTA3, TBM080658-MRI (EEG-fMRI), PhD Grants; IBBT Belgian Federal Science Policy Office: IUAP P6/04 (DYSCO, 'Dynamical systems, control and optimization', 2007-2011); ESA AO-PGPF-01, PRODEX (CardioControl) C4000103224. EU: RECAP 209G within INTERREG IVB NWE programme, EU HIP Trial FP7-HEALTH/ 2007-2013 (n° 260777) (NeuroMath (COST-BM0601) Other: BIR&D Smart Care.

A. C. is with the Electronic Engineering Department, ESAT/SCD SISTA, Katholieke Universiteit Leuven, Leuven, Belgium. He is also with the IBBT Future Health Department, Katholieke Universiteit Leuven, Leuven, Belgium (phone: +32 16 321067; e-mail: alexander.caicedodorado@esat.kuleuven.be).

I. T. and M.D. P. are members of the Biomedical Optics Research Laboratory at the Medical Physics and Bioengineering Department, University College London, London, UK (e-mail: iliastac@medphys.ucl.ac.uk and mpapa@medphys.ucl.ac.uk, respectively).

S. V.H. is with the Electronic Engineering Department, ESAT/SCD SISTA, Katholieke Universiteit Leuven, Leuven, Belgium. She is also with the IBBT Future Health Department, Katholieke Universiteit Leuven, Leuven, Belgium (e-mail: sabine.vanhuffel@esat.kuleuven.be).

the major neck vessels – right common carotid artery (RCCA) and internal jugular vein (IJV). Blood drains from the patient and gets oxygenated externally by the ECMO circuit and returns back to the patient. VA ECMO bypasses both the heart and lungs and provides cardiac and respiratory support. Venovenous (VV) ECMO bypasses only the lungs and in this case the patient has only one double lumen cannula inserted in the IJV. VV ECMO does not provide cardiac support. Patients undergoing ECMO often have periods of haemodynamics instability, hypoxia and/or hypercapnia; in addition, physiological changes caused by the ECMO procedure itself may alter the cerebral autoregulation mechanisms due to multi-factorial reasons such as heparinization, hemodilution and reduced arterial pulsatility [1]; in consequence ECMO patients have increased risk for brain injury. Several studies have described changes in the cerebral haemodynamics before, during and after ECMO procedure. Liem et al. reported that mean arterial blood pressure (MABP), arterial oxygen saturation (SaO₂), transcutaneous partial pressure of oxygen (tcpO₂) and transcutaneous partial pressure of CO₂ (tcpCO₂) were some of the variables that better explained changes in total haemoglobin (HbT). Ejike et al. reported no significant correlation between changes in ECMO flow and regional oxygen saturation (rScO₂) and a negative correlation between rScO₂ and pCO₂. Papademetriou et al. described oscillations in brain and peripheral haemodynamics during changes in ECMO flow, as measured with near-infrared spectroscopy (NIRS), and its use as a marker of cerebral autoregulation [3, 4]. Studies about the coupling between systemic and haemodynamic variables have been performed by means of regression models [2, 5]. Although these approaches seem to provide good results they can be highly affected by the presence of multi-collinear variables and non-stationarities. In a previous work [6] we aimed to study the interactions of these variables by means of Canonical Correlation Analysis (CCA). Although CCA provides a strong theoretical framework to study the coupling between multivariable datasets, the results are difficult to analyze which reduce its clinical value.

Subspace projections methods, on the other hand, address straightforwardly this problem producing results that are not only easy to interpret mathematically but also clinically. The main goal of subspace projection techniques in signal processing is to mitigate the influence of noise in a signal of interest. Thus, orthogonal subspace projection (OrSP) and oblique Subspace Projection (OSP) aim to reduce orthogonal

and oblique noise, respectively; where the noise can be due to measurement noise or contamination by other signals dynamics. In this study we aim to decouple the dynamic of the systemic variables (SV) from the cerebral-peripheral haemodynamic variables (CHV, PHV) by means of OrSP and OSP in combination with the discrete wavelet decomposition of the SV. In addition the strength of the coupling was quantified using features extracted from the decoupled signals.

II. METHODS

A. Data

Measurements from a patient, 3 days old, undergoing ECMO procedure were used in this study. A dual channel near infrared spectroscopy (NIRS) system (NIRO 200, Hamamatsu Photonics KK) was used to measure changes in oxy- and deoxy- haemoglobin concentrations (HbO₂ and HHb), and tissue oxygenation index (TOI), which is calculated as HbO₂/(HbO₂+HHb), using spatially resolved spectroscopy. NIRS data were collected at a frequency of 6Hz. Channel 1 was placed on the forehead in order to assess cerebral haemodynamics, while channel 2 was placed on the calf to assess peripheral haemodynamics. Systemic data: mean arterial blood pressure (MABP), end-tidal CO₂ (EtCO₂), heart rate (HR), core temperature (Core T) and arterial oxygen saturation SaO₂; were continuously measured in real time at the bedside (Intellvue MP70, Philips Medical Systems). MABP was obtained invasively from a radial artery. SaO₂ was obtained from a pulse oximeter placed on the toe of the patient. MABP was recorded at 125Hz while EtCO₂ was recorded at 62.5Hz. All data were downsampled to 1Hz and artifacts were removed manually by using interpolation.

In figure 1 the systemic and NIRS measurements from the patient are shown. The data was collected during changes in the ECMO flow. The ECMO flow was initially decreased from baseline level (100%) in steps of 10% down to 70%, and then it was increased, following the same profile, until baseline level was reached.

B. Subspace Projections

In linear algebra a projection onto a subspace can be performed by the use of a projection matrix. A projection matrix is then an operator that maps any vector in a subspace spanned by its column space. A general overview of subspace projections and its properties can be found in [7]. In subspace projection techniques the goal is to find a projection matrix that performs this task. Let the matrix X of size $m \times n$ be composed of the vectors $\{x_1, x_2, \dots, x_n\}$, with $x_i \in \mathcal{R}^m$, in its columns. Assuming that X is full rank (rank = n , with $m > n$) the vectors $\{x_1, \dots, x_n\}$ form a basis for the column space of X , $C(X)$. Given X , the orthogonal projection matrix $P = X(X^T X)^{-1} X^T$, is the matrix that projects any vector $y \in \mathcal{R}^m$ in $C(X)$. This projection is calculated as $y_X = P y$. Whilst its projection in the orthogonal subspace of $C(X)$, namely $C(X^\perp)$ or the null space of $X^T N(X^T)$, is $y_X^\perp = (I - P)y$, with $y = y_X + y_X^\perp$.

An oblique projection, on the other hand, is a projection that is carried out along oblique subspaces. In the case of an orthogonal projection, the projection was performed along $C(X)$ and $N(X^T)$. Those 2 subspaces were completely defined by the data in X . However, for an oblique projection a second reference is needed, as the projection should be performed parallel to this reference subspace.

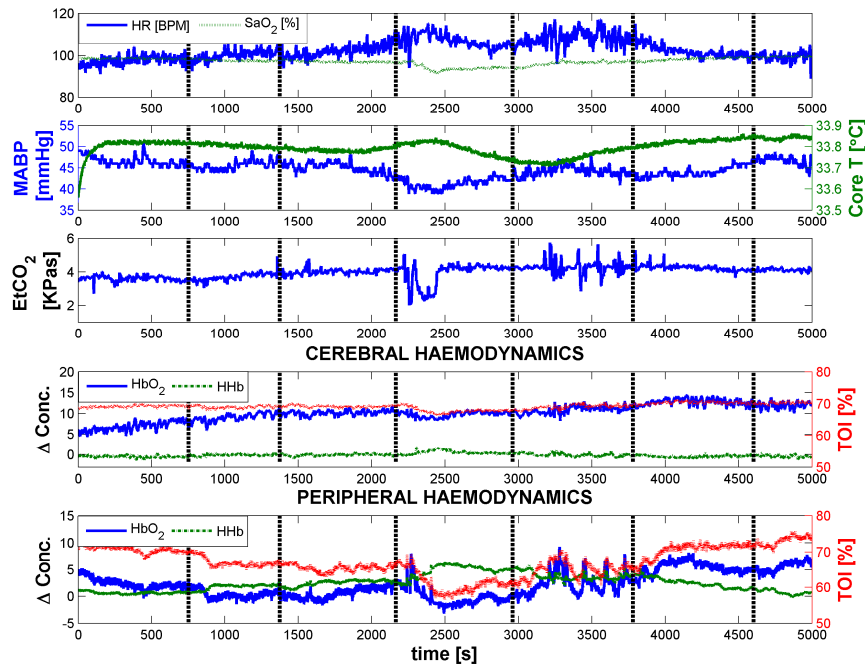


Figure 1. Systemic and Haemodynamic variables measured from the patient. The dotted vertical Lines represent the changes in the ECMO flow. The flow was first decreased from baseline level (100%) up to 70% in steps of 10%, afterwards it was returned to the baseline level following the same profile.

Let a matrix \mathbf{Z} be composed of linearly independent vectors $\{z_1, z_2, \dots, z_p\}$, $z_i \in \mathcal{R}^m$, then the projection matrix that projects a vector y in $C(\mathbf{Z})$ along $C(\mathbf{X})$, denoted by $\mathbf{E}_{\mathbf{Z}\mathbf{X}}$, and the projection matrix that projects a vector y in $C(\mathbf{X})$ along $C(\mathbf{Z})$, denoted by $\mathbf{E}_{\mathbf{X}\mathbf{Z}}$, are given by:

$$\mathbf{E}_{\mathbf{Z}\mathbf{X}} = \begin{bmatrix} \mathbf{Z} & \mathbf{0} \\ \mathbf{X}^T \mathbf{Z} & \mathbf{X}^T \mathbf{X} \end{bmatrix}^{-1} \begin{bmatrix} \mathbf{Z}^T \\ \mathbf{X}^T \end{bmatrix} \quad (1)$$

$$\mathbf{E}_{\mathbf{X}\mathbf{Z}} = \begin{bmatrix} \mathbf{0} & \mathbf{X} \\ \mathbf{X}^T \mathbf{Z} & \mathbf{X}^T \mathbf{X} \end{bmatrix}^{-1} \begin{bmatrix} \mathbf{Z}^T \\ \mathbf{X}^T \end{bmatrix} \quad (2)$$

The geometrical interpretation of subspace projections can be seen in figure 2.

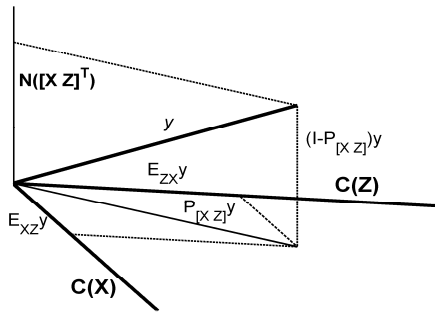


Figure 2. Geometrical interpretation for orthogonal and oblique projections.

C. Decoupling Algorithm

The problem was addressed in two different ways. On one hand, the projection of the cerebral and peripheral haemodynamic variables (CHV, PHV) in the subspace spanned by the systemic variables (SV) decomposes CHV and PHV in a part that is linearly related to SV and a part that is orthogonal to it. The orthogonal part can be interpreted as the part of the haemodynamic variables (HV) that is related to measurement noise, not measured variables and nonlinear coupling with SV. On the other hand, the CHV and PHV can be projected on each one of the SV by calculating the corresponding oblique projection matrices; where the matrix \mathbf{Z} , in (1) and (2), corresponds to the signal on which we would like to project the data and the matrix \mathbf{X} to the remaining SV. However, if raw signals are used to define $C(\mathbf{X})$ the projection matrices will be highly sensitive to non-stationarities and high noise levels. Therefore, a change of the raw SV signals by the wavelet transform of the SV, as basis for $C(\mathbf{X})$, is proposed. The use of the wavelet transform not only mitigates the effect of noise in the projections but also, intuitively, introduces the effects of non-stationarities. In this study we used 5th level discrete wavelet decomposition, with Daubechies 4 as mother wavelet. Moreover, in order to account for possible coupling delays, the wavelet coefficients of SV and its delayed versions were included in the matrix \mathbf{X} . In this study a delay

of three samples was used. The use of the delays can be interpreted as imposing a model structure in the projection matrices. In addition, the ratios between the power of the projected and original signals, were computed as a measure of the coupling between the variables. In summary the algorithm is reduced to the following steps:

ALGORITHM

Input: Systemic Variables (SV) ($m \times n$) and Haemodynamic Variables (HV) ($m \times d$).

Output: Projected HV ($m-3 \times dxn$), residuals ($m-3 \times d$) and ratios between the power of the projections and the original signals ($2 \times d$).

1. Subtract the mean value from each SV and HV.
2. Compute a 5th level discrete wavelet transform of each SV using the db4 as mother wavelet.
3. Delay the signals resulting from the discrete wavelet transform by 1, 2 and 3 samples.
4. Concatenate all the signals in a matrix \mathbf{X} . If there are n SV and their length is m , the final matrix \mathbf{X} should be of dimensions $(m-3) \times (5*n*3)$, with $m-3 \gg 5*n*3$.
5. Compute the OrSP matrix for the matrix \mathbf{X} , and project the HV in $C(\mathbf{X})$.
6. From this projection compute the ratios between the power of the projected and the original HV.
7. Compute the OSP matrix for each SV, as explained in equations 1 and 2. Project the data in each one of the subspaces defined by each SV.
8. Normalize all the oblique projections by the power of the orthogonal projection of the HV in $C(\mathbf{X})$.
9. From the projected signals compute the ratio between the projected variable and the original signal.

The different ratios calculated in the algorithm will be used as a measure of the strength of the coupling between CHV/PHV and SV, namely P_C and P_P respectively. The ratios can be interpreted as the amount of power in the CHV/PHV due to the SV in total, in case of an orthogonal projection, or separately, in case of oblique projection. The ratio P_C/P_P can be used as a monitoring variable to assess the status of the mechanisms that regulates cerebral haemodynamics.

III. RESULTS

In figure 3, the decomposition of the cerebral and peripheral TOI in the components corresponding to each SV is shown. The peripheral TOI is more affected than the cerebral TOI by variations in SV; this might be due to intrinsic mechanisms that regulate cerebral haemodynamics. The ratio P_C/P_P was 0.62 for HbO₂, 0.058 for HHb and 0.045 for TOI. In table 2 the ratios between the powers of the projected CHV/PHV in the SV are displayed. These ratios reveal the SV that affect at most the HV. This table shows that variations in SaO₂ possess the highest impact in the variations of CHV and PHV. However, its influence is more pronounced in the peripheral haemodynamics. In addition EtCO₂ appears to have a higher impact in the cerebral than in the peripheral haemodynamics.

IV. DISCUSSION

OrSP and OSP were able to decompose the CHV/PHV in a series of components related to each SV. This approach is useful as it serves as a basis for the quantification of the coupling between the haemodynamics and the systemic variables. By calculating the ratios between the power of the components in the decomposed signal and the original signal the strength of the coupling was assessed. By including wavelets as a basis for the subspace of the systemic variables the non-stationary effects are taken into account; however, further studies are needed in order to validate these results and evaluate their clinical impact. In addition, the effect of nonlinear coupling should be further studied, as it is not included in the current analysis. In summary, in this study we have presented a way to decouple the influence of SV in CHV and PHV. This information may yield high clinical impact as it can alert the clinician which variable has the highest impact in the cerebral haemodynamics.

REFERENCES

[1] K. Liem, J. Hopman, B. Oesenburg, A. De Haan, C. Festen, and L. Kollee, "Cerebral Oxygenation and hemodynamics during induction of extracorporeal membrane oxygenation as investigated by near infrared spectrophotometry". *Pediatrics* 93:555-561, 1995.

[2] J. Ejike, K. Schenkeman, K. Seidel, C. Ramamoorthy, and J. Roberts. "Cerebral oxygenation in neonatal and pediatric patients during veno-arterial extracorporeal life support". *Pediatric Critical Care Medicine* 7:154-158, 2006.

[3] M.D. Papademetriou, I. Tachtsidis, T.S. Leung, M.J. Elliott, A. Hoskote, C.E. Elwell. "Cerebral and Peripheral Tissue Oxygenation in Children Supported on ECMO for Cardio-Respiratory Failure". *Adv.Exp.Med.Biol* 662:447-53, 2010.

[4] M.D. Papademetriou, I. Tachtsidis, M. Banaji, M.J. Elliott, A. Hoskote, C.E. Elwell. "Optical topography to measure variations in regional cerebral oxygenation in an infant supported on veno-arterial extra-corporeal membrane oxygenation". *Adv Exp Med Biol.* 737:71-6, 2012.

[5] M.M. Tisdal, C. Taylor, I. Tashtsidis, T.S. Leung, C.E. Elwell, and M. Smith. "The effect on Cerebral Tissue Oxygenation Index of Changes in the Concentrations of Inspired Oxygen and End-Tidal Carbon Dioxide in Healthy Adult Volunteers". *Anesth Anal* 109(3): 906-913, 2009.

[6] A. Caicedo, M.D. Papademetriou, C.E. Elwell, A. Hoskote, M.J. Elliott, S. Van Huffel, and I. Tachtsidis. "Canonical Correlation Analysis in the Study of Cerebral and Peripheral Haemodynamics Interrelations with systemic Variable sin Neonates Supported on ECMO". *Adv. Exp. Med. Biol. Waiting for publication.*

[7] R.T. Behrens and L.L. Scharf. "Signal Processing Applications of Oblique Projection Operators". *IEEE Trans. Signal Process.* 42(6) pp. 1413-1423, June, 1994.

	Peripheral Haemodynamics						Cerebral Haemodynamics					
	HR	MABP	Core T	SpO ₂	EtCO ₂	Flow	HR	MABP	Core T	SpO ₂	EtCO ₂	Flow
HbO ₂	2.23	15.13	1.68	38.20	4.02	5.57	5.43	2.07	4.24	26.63	17.89	8.83
HHb	5.03	7.55	0.79	68.09	9.31	1.43	0.41	4.76	4.25	48.70	1.39	4.44
TOI	0.49	7.28	0.56	70.57	0.37	9.63	1.72	2.41	0.32	71.61	4.63	0.46

Table 1. Percentage of power in the corresponding Peripheral or Cerebral Haemodynamic variable (left-column) due to the systemic variables (second row).

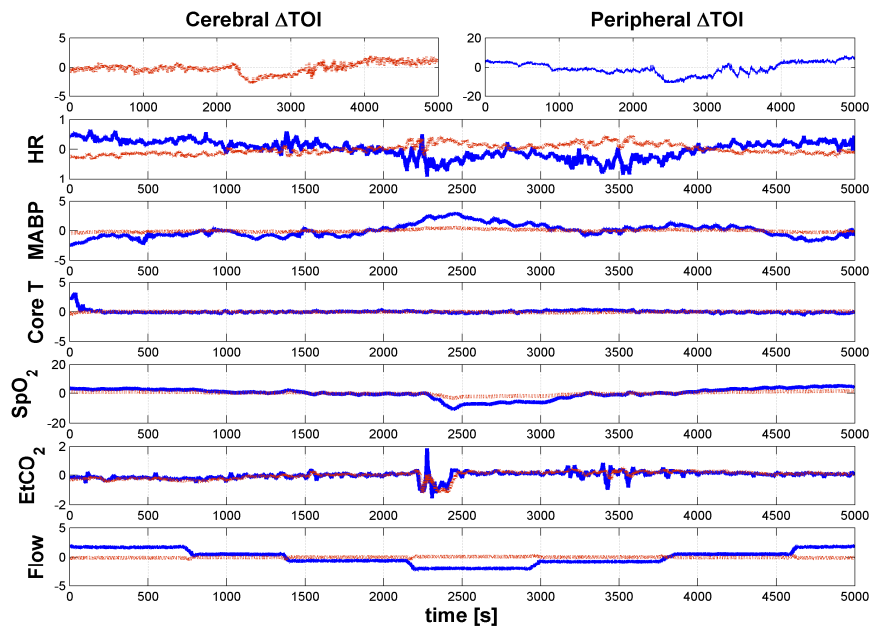


Figure 3. Decomposition of the Cerebral and Peripheral TOI in the components related to each one of the systemic variables under analysis. In red the decomposition for the cerebral TOI is shown, whilst blue represents the decomposition for peripheral TOI.